MATERIALS INNOVATION MEMORANDUM

To:	Zachary Combs
From:	Ryan Waldheim
CC:	James Benson, Michael Regula, Doug Barr
Subject:	**LS-28591: Characterization of Targray NMC532 and NMC811**
Date:	November 8, 2019

SUMMARY

As Birla Carbon expands its research in the energy storage applications, preliminary reference data and novel analysis techniques will be required for many materials new to the Marietta laboratory. A previous study (LS-28245) sought to study to impact of different carbon black colloidal properties on the resistivity of a resulting anodes. The inherently conductive nature of graphite made the resistivity changes due to carbon black additives difficult to isolate. A current study seeks to perform a similar methodology on cathodes (LS-28575) using $Li(Ni_{0.5}Mn_{0.3}Co_{0.2})O_2$ (NMC532), which has a higher bulk resistivity. This active material is new to Birla Carbon therefore its properties should be validated and tested, using both mature and new techniques, against the specifications provided by its manufacturer, Targray Technology International Inc.

SAMPLE IDENTIFICATION

A-Number	Sample Description
A-93192	Targray NMC532 (SNMC03010)
A-93193	Targray NMC811 (SNMC03008)

SUMMARY OF BULK TECHNIQUE RESULTS

The specifications provided by Targray can be found in the **Appendix** for both the NMC532 (SNMC03010) and NMC811 (SNMC03008) samples.

Traditional powder properties are listed in **Table 1**. A slight deviation in surface area is observed; however, the particle size of the NMC samples is too large for reliable BET surface area measurements using nitrogen. A future BET surface area experiment will be executed using larger adsorption gases, such as argon or krypton. Densities are similar to the manufacturer specifications.

1800 WEST OAK COMMONS COURT, MARIETTA, GA 30062-2253
PHONE 770-792-9400 • FAX 770-792-9631 • www.birlacarbon.com

Table 1: Traditional powder properties.

Test	Units	A-93192 Targray NMC532	A-93193 Targray NMC811
NSA	m^2/g	0.1	0.3
As Is Density	g/cm^3 (lb/ft^3)	1.71 (106.7)	2.14 (133.5)
Tap Density	g/cm^3 (lb/ft^3)	2.41 (150.3)	2.61 (162.8)
He Density	g/cm^3	4.69	4.63

X-Ray Diffraction (XRD) spectra patterns match strongly with values reported in literature (**Figure 1**), with a likely contaminant of graphite in the sample indicated by the peak present at 27º in both samples, as shown in **Figure 2**.

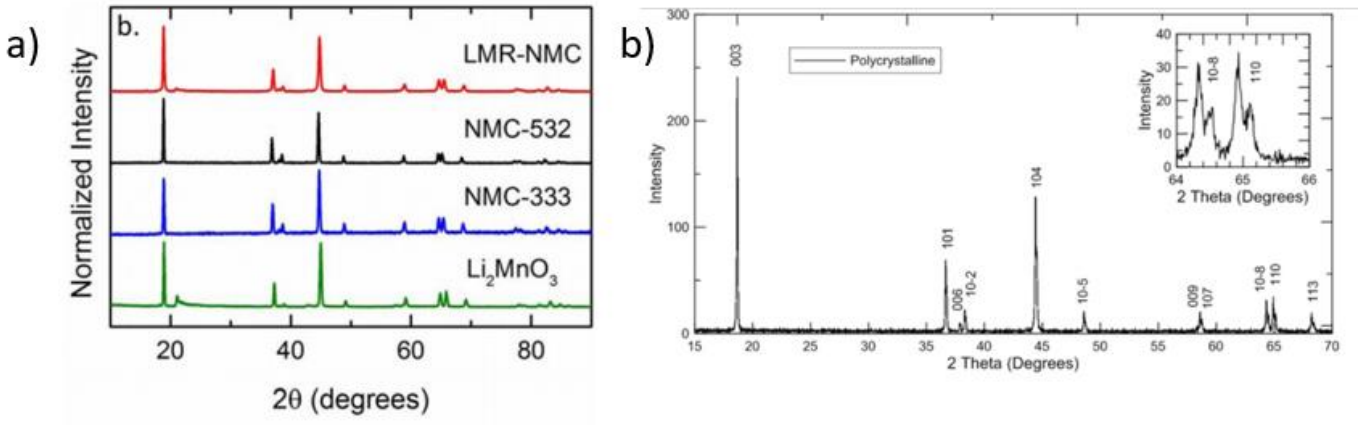

Figure 1: Reference NMC532 XRD (a) data (Ruther, Callender, Martha, & Nanda, 2015), and NMC811 and XRD (Weber, Fell, Dahn, & Hy, 2017) (b).

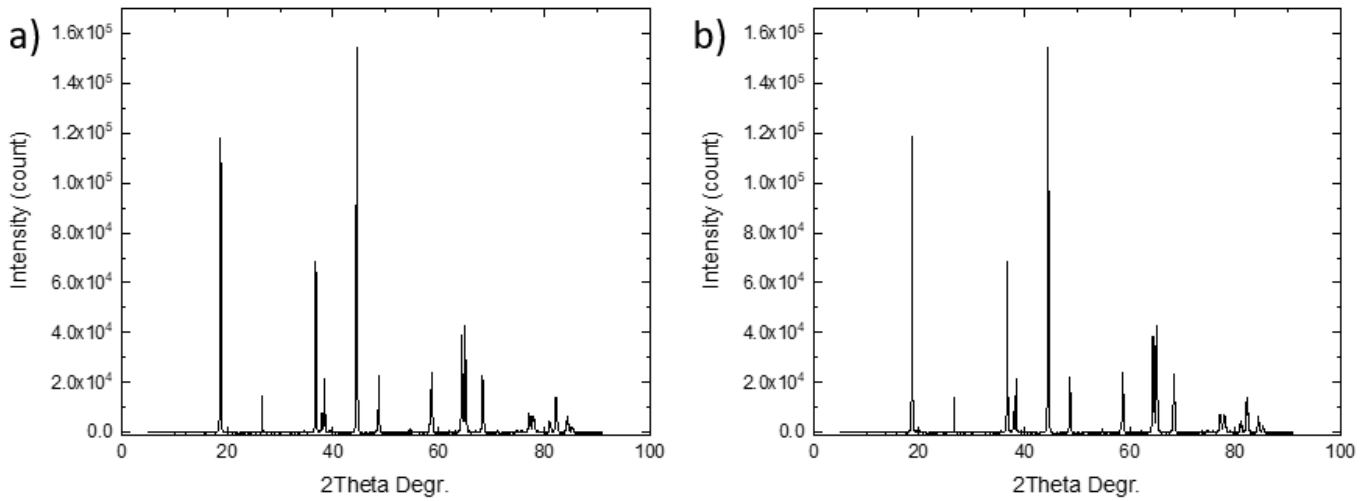

Figure 2: XRD spectrum for NMC532 (a) and NMC811 (b). The peak at 27º is indicative of a graphite contaminant likely present in the sample holder.

To obtain an accurate particle size distribution using the Horiba Partica particle size analyzer (PSA), the refractive index of the sample must be known. At the time of writing, the refractive indices of NMC532 and NMC811 are unknown. Recalibration of the particle size distribution calculation at difference refractive indices is possible after the sample has been measured, therefore both samples were initially measured using the refractive index of graphite. Recalibration was then done using the Real Refractive Index Wizard in the Horiba LA-960 software by testing the refractive indexes of other, known transition metal oxides, as listed in **Table 2**. The refractive indexes for the transition metals were taken from RefractiveIndex.info. The refractive index appears to have little impact on the resulting particle size distribution, as shown in **Figure 4**. Each real refractive index was also measured using ranging values of the imaginary refractive index, to get a sense of the complete, complex refractive index's influence on the particle size distribution.

To further this study, a significantly wider range of refractive indexes were taken, ranging from 0.01 to 10, and the particle size distribution was recalibrated in the same manner. Each recalculation included an imaginary refractive index value of 0.1. The refractive index still appeared to have very little influence on the resulting particle size distribution, as seen in **Figure 5**. Though proven to not influence the distribution on the scale of the NMC particles, the approximately 0.5 µm variance in average particle size with refractive index would be critical to minimize in measuring much finer material, such as carbon black.

Table 2: Refractive indices of transition metal oxides used for calibration of the NMC particle size distributions.

Transition Oxide	Refractive Index
Ta_2O_5	2.16
MoO_3	2.28
NiO	2.30
Nb_2O_5	2.53
TiO_2	2.87

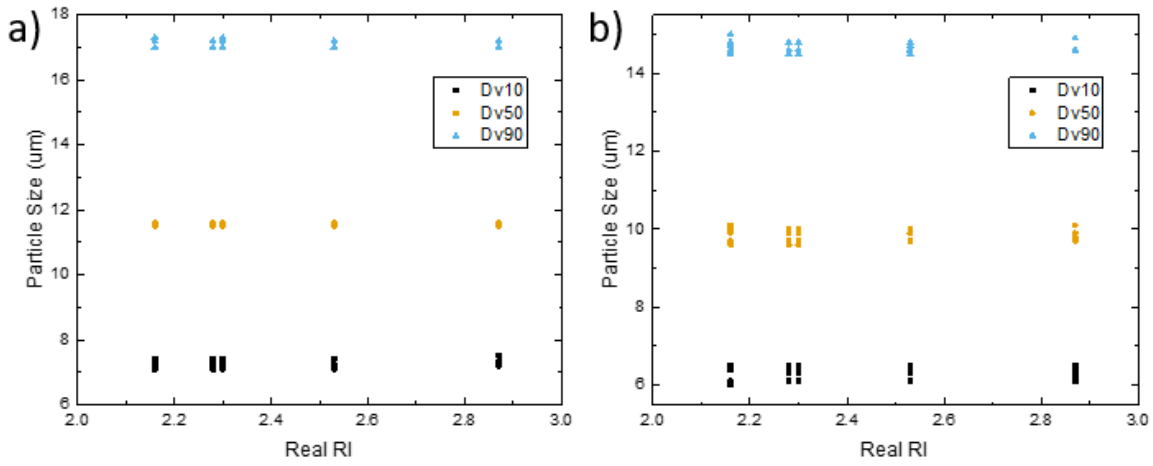

Figure 3: Particle size distribution data recalculated for various transition metal oxides for NMC532 (a) and NMC811 (b), with five imaginary refractive indexes calculated at each real index: 0, 0.01, 0.1, 1, and 10. Little deviation observed.

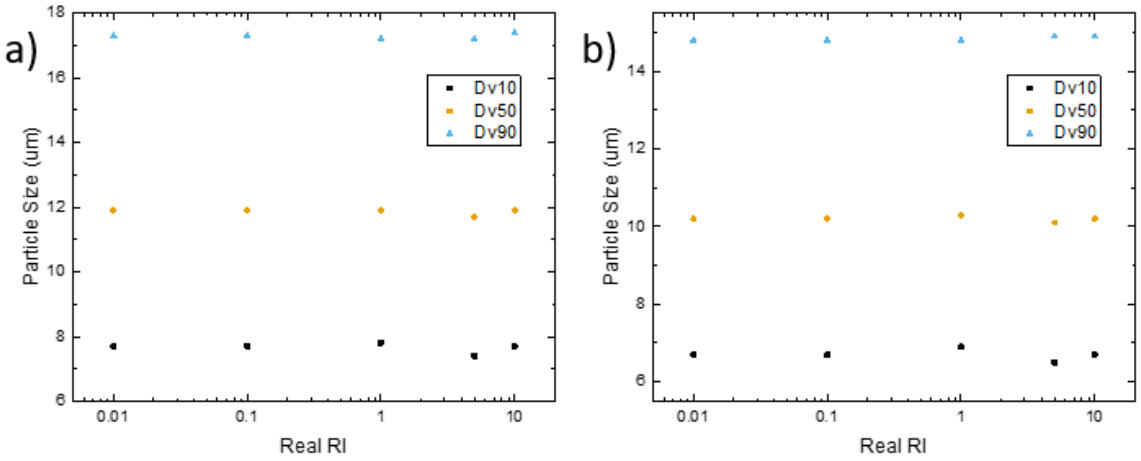

Figure 4: Particle size distribution data taken at "extreme" values of the real refractive index (0.01, 0.1, 0.99, 5, and 10) with the imaginary index held at 0.1 for both NMC532 (a) and NMC811 (b). Little deviation observed.

The resulting particle size distribution, shown in **Table 3**, was taken using the real refractive index for NiO (2.30) with an imaginary value of 0.1 as representative of the median value tested. Resulting distributions are a few micron smaller in average particle size, but contain tighter span factors than those reported by Targray.

Table 3: Particle Size Distribution

Test	A-93192 Targray NMC532	A-93193 Targray NMC811
D_v10	6.1	7.1
D_v50	9.6	11.5
D_v90	14.6	17.2
Relative Span Factor (RSF)	0.89	0.88

The particle size distributions of both samples was confirmed with scanning electron microscopy (SEM) images, as seen in **Figure 6**. The NMC particles have a distinct rough surface morphology (532 roughness greater tha 811) compared to other battery materials that have been previously evaluated such as graphite.

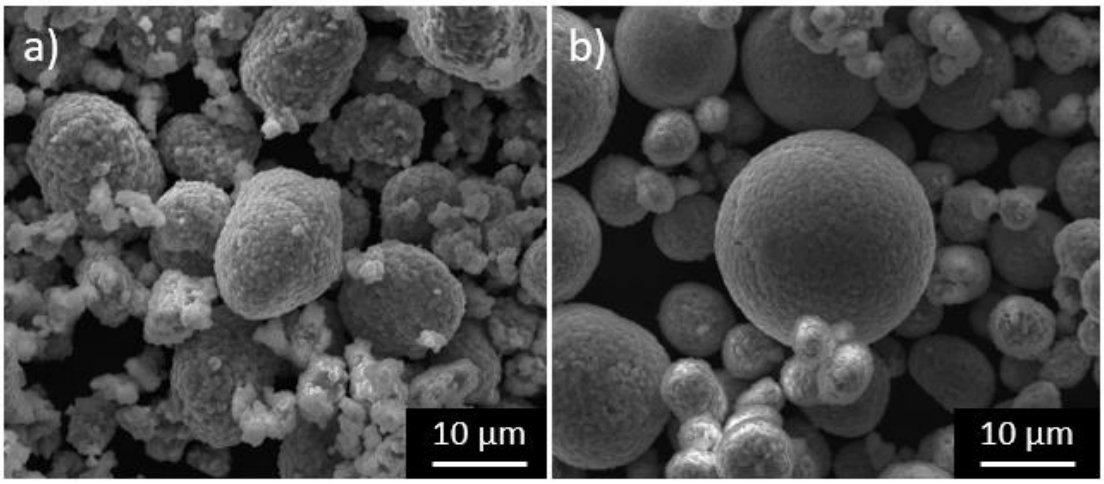

Figure 5: SEM images of NMC532 (a) and NMC811 (b) particles. Particles appear to agree with the particle size distribution data as calculated from the particle size analyzer.

REFERENCES

Jung, R., Morasch, R., Karayaylali, P., Phillips, K., Maglia, F., Stinner, C., . . . Gasteiger, H. A. (2018). Effect of Ambient Storage on the Degradation of Ni-Rich Positive Electrode Materials (NMC811) for Li-Ion Batteries. *Journal of the Electrochemical Society*, A132-A141.

Ruther, R. E., Callender, A. F., Martha, S. K., & Nanda, J. (2015). Raman Microscopy of Lithium-Manganese-Rich Transition Metal Oxide Cathodes. *Journal of the Electrochemistry Society*, A98-A102.

Weber, R., Fell, C. R., Dahn, J. R., & Hy, S. (2017). Operando X-ray Diffraction Study of Polycrystalline and Single-Crystal LixNi0.5Mn0.3Co0.2O2. *Jounral of the Electrochemical Society*, A2992-A2999.

APPENDIX

NMC Product Line

Product Code		SNMC 03001	SNMC 03002	SNMC 03010	SNMC 03009	SNMC 03006	SNMC 03008
Material		NMC 333	NMC 532			NMC 622	NMC 811
Physico-chemical properties	D10/um	4.2	6.2	5	3.7	7	6.7
	D50/um	6.5	11	10.1	6.4	10	13.8
	D90/um	11	20.7	18.2	10.7	19	25.1
	BET/m2/g	0.48	0.24	0.45	0.51	0.28	0.49
	TD/g/cm3	2.2	2.63	2.25	1.78	2.5	2.31
	PH	11.1	11.56	11.5	11.15	11.65	12.13
	Li2CO3/%	0.05	0.08	0.13	0.08	0.25	0.64
	LiOH/%	0.03	0.09	0.10	0.02	0.13	0.43
Electro-chemical data 2.8 – 4.25V	Capacity/ mAh.g-1	154.8	166.9	166.1	187.0@4.5V	175.8	203.4@4.3V
	Efficiency/%	88.8	89.3	88.1	86.0@4.5V	90.3	88.4@4.3V
	Rate capacity retention/%	94.8	93.4	94.9	94.3@4.5V	93.4	94.0@4.3V
	Cycle capacity retention @50 cycles/%	98.3	95.6	99.2	96.1@4.5V	98.1	93.4@4.3V

NCA Product Line

Product Code		A8E	SNCA04001
Material		NCA(80%Ni)	
Physico-chemical properties	D10/um	4.6	≥3.0
	D50/um	10.9	8-13
	D90/um	18.9	≤30.0
	BET/m2/g	0.33	0.35
	TD/g/cm3	2.7	2.6
	PH	12.32	11.5-12.5
	Li2CO3/%	0.42	0.45
	LiOH/%	0.44	0.36
Electro-chemical data 2.8 – 4.25V	Capacity/ mAh.g-1	199.6@4.3V	200.5@4.3V
	Efficiency/%	89.4@4.3V	91.4@4.3V
	Rate capacity retention/%	93.5@4.3V	93.5@4.3V
	Cycle capacity retention @50 cycles/%	95.6@4.3V	94.8@4.3V